Tunable emission, concentration quenching and crystallographic sites of Eu^{2+} in $Sr_3Y(PO_4)_3$*

ZHANG Zi-cai (张子才)[1], **XU Shu-chao** (徐书超)[1], **LI Pan-lai** (李盼来)[1], **WANG Zhi-jun** (王志军)[1]**, **SUN Jiang** (孙江)[1]**, **YANG Zhi-ping** (杨志平)[1], and **PANG Li-bin** (庞立斌)[1,2]**

1. College of Physics Science & Technology, Hebei University, Baoding 071002, China

2. Department of Foreign Language Teaching and Research, Hebei University, Baoding 071002, China

(Received 18 July 2014)

A series of $Sr_3Y(PO_4)_3:Eu^{2+}$ samples are synthesized by the high temperature solid-state method. $Sr_3Y(PO_4)_3:Eu^{2+}$ shows an asymmetrical emission band under excitation of 350 nm. The emission peaks at 426 nm and 497 nm are assigned to the nine-coordination Eu^{2+} and six-coordination Eu^{2+}, respectively. The effects of Eu^{2+} doping content on the emission intensity and color are observed, and the concentration quenching effect is also observed. For two different Eu^{2+} luminescence centers, the quenching mechanisms are dipole-dipole interaction and quadrupole-quadrupole interaction, respectively. And the critical distance of energy transfer is calculated by concentration quenching and turns out to be about 3.67 nm. The results above show that the asymmetrical emission band of $Sr_3Y(PO_4)_3:Eu^{2+}$ comes from two different Eu^{2+} luminescence centers in the lattice.

Document code: A **Article ID:** 1673-1905(2014)06-0447-4

DOI 10.1007/s11801-014-4138-z

Eu^{2+} has many applications because its d-f emission is partly allowed, resulting in high emission intensity[1]. The emission energy shows a strong dependence on crystal field and covalence, and the Eu^{2+} doped phosphors usually have a strong absorption in the spectra from ultraviolet (UV) to visible region and exhibit broad emission bands covering the color region from blue to red[2]. Especially, the host compound has several crystallographic sites, which can serve as a host for luminescence materials with several centers when Eu^{2+} is doped into the compound, and can lead to the different emission colors of Eu^{2+} in a single compound[3]. Therefore, Eu^{2+} doped phosphors have applications in several fields, such as light emitting diodes (LEDs), plasma display panels (PDPs) and field emission displays (FEDs)[4-6].

$M^I_3M^{II}(PO_4)_3$ (M^I=Ca, Sr, Ba and Pb, and M^{II}=La, Y, Sc, Bi, Tb and In) with eulytite-type structure can provide several crystallographic sites of cation, so they have attracted extensive attention as host materials for Eu^{2+}, Ce^{3+}, etc[7-9]. For example, the luminescence and the energy transfers of Eu^{2+} to Mn^{2+}, Tb^{3+} to Mn^{2+} and Ce^{3+} to Tb^{3+} in $M^I_3M^{II}(PO_4)_3$ have been extensively studied[7-9]. Moreover, the near-infrared quantum cutting in $Sr_3Gd(PO_4)_3:Eu^{2+}$, Yb^{3+} has been also reported[10]. For $Sr_3Y(PO_4)_3$, there are two sites of Sr^{2+} in the host, the first Sr^{2+} coordinates with nine oxygen atoms while the second Sr^{2+} coordinates with six oxygen atoms. Therefore, $Sr_3Y(PO_4)_3$ may offer different luminescence centers to Eu^{2+}, and produce the tunable emission. In this paper, we thoroughly discuss the tunable emission, concentration quenching and crystallographic sites of Eu^{2+} in $Sr_3Y(PO_4)_3$.

A series of $Sr_{3-x}Y(PO_4)_3:xEu^{2+}$ were synthesized by high temperature solid-state reaction method, where x represents the molar ratio of Eu^{2+}. The initial materials, including $SrCO_3$ (A.R.), Y_2O_3 (A.R.), $NH_4H_2PO_4$ (A.R.) and Eu_2O_3 (99.99%), were weighted in stoichiometric proportion, thoroughly mixed and ground by an agate mortar and pestle for more than 30 min until they were uniformly distributed. The obtained mixtures were heated at 1 350 °C for 4 h in crucibles along with reducing atmosphere (5%H_2/95%N_2), and then naturally cooled to room temperature. In order to measure the characteristics of the phosphor, the samples were ground into powder.

The phase formation was determined by X-ray diffraction (XRD) by a Bruker AXS D8 advanced automatic diffractometer (Bruker Co., German) with Ni-filtered Cu Kα radiation (λ=0.154 06 nm), and a scan rate of 0.02°/s is applied to record the patterns in 2θ range from 20° to 90°. The excitation and emission spectra were detected by a fluorescence spectrophotometer (Hitachi F-4600) with the exciting source of Xe lamp at 450 W. The steady time resolved photoluminescence (PL) spectra were de-

* This work has been supported by the National Natural Science Foundation of China (No.50902042), the Natural Science Foundation of Hebei Province of China (Nos.A2014201035 and E2014201037), and the Education Office Research Foundation of Hebei Province of China (Nos.ZD2014036 and QN2014085).

** E-mails: wangzj1998@sohu.com; lipanlai@sohu.com; lizhibin268@sohu.com

tected by a FLS920 fluorescence spectrometer with the exciting source of Xe lamp at 450 W. The curve fitting is performed on the PL decay curves to confirm the PL decay time. The Commission International de I'Eclairage (CIE) chromaticity coordinates of samples were measured by a PMS-80 spectra analysis system. All measurements were carried out at room temperature.

The phase formation of $Sr_{3-x}Y(PO_4)_3$:xEu^{2+} is determined by the XRD pattern, and a similar diffraction pattern is observed for each sample. As a representative, Fig.1 shows the XRD patterns of $Sr_{2.99}Y(PO_4)_3$:$0.01Eu^{2+}$. Comparing the diffraction data with the standard JCPDS card (No.44-0320), the results indicate that there is no difference between $Sr_3Y(PO_4)_3$:Eu^{2+} and the pure $Sr_3Y(PO_4)_3$. It means that the phase formation of $Sr_3Y(PO_4)_3$ is not influenced by a little amount of Eu^{2+}. $Sr_3Y(PO_4)_3$ has a cubic crystal structure with a space group of I-43d(220), and the cell parameters are a=b=c=1.010 91 nm. Sr^{2+}/Y^{3+} pairs are disordered on a single crystallographic site, while the oxygen atoms of the phosphate groups are distributed at three partially occupied sites[11]. On basis of the effective ionic radii of cations with different coordination numbers (CNs), Eu^{2+} may prefer to occupy the sites of Sr^{2+} since the ionic radius of Eu^{2+} is similar to that of Sr^{2+}[12].

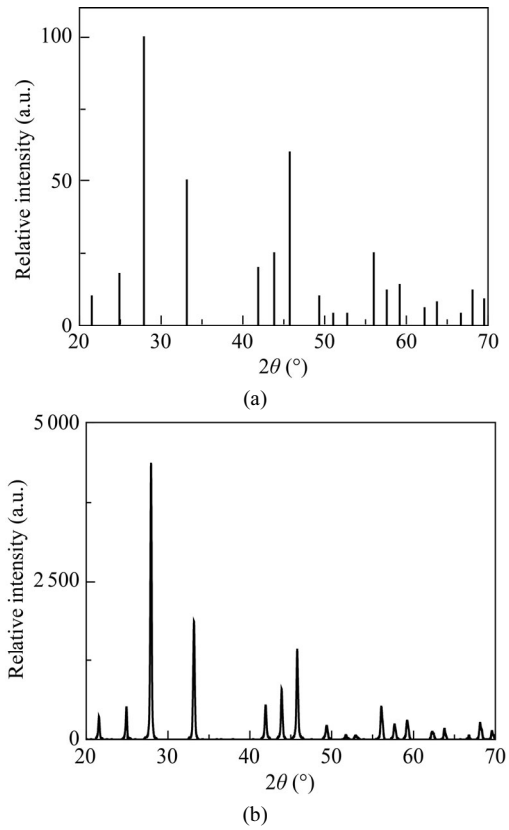

Fig.1 XRD patterns of (a) $Sr_3Y(PO_4)_3$ (standard JCPDS card No.44-0320) and (b) $Sr_3Y(PO_4)_3$:$0.01Eu^{2+}$

Fig.2 shows the emission and excitation spectra of $Sr_3Y(PO_4)_3$:$0.01Eu^{2+}$. Under the radiation excitation at 350 nm, $Sr_3Y(PO_4)_3$:Eu^{2+} exhibits an asymmetrical emission band with a maximum at about 500 nm, which is ascribed to the electric dipole allowed transition of Eu^{2+} from the lowest level of 5d excited state to 4f ground state. The asymmetrical emission band means that two overlapping emission bands may exist, and the present host lattice has an available family of sites for Eu^{2+} ions attributed to the disorder in the lattice. In order to analyze the observed phenomena, the emission spectrum of $Sr_3Y(PO_4)_3$:Eu^{2+} is decomposed into two Gaussian profiles with peaks at 426 nm (23 474 cm^{-1}) and 497 nm (20 121 cm^{-1}), respectively. For the emissions at 426 nm and 497 nm, the corresponding excitation spectra present the different profiles with the peaks locating at 333 nm and 342 nm, respectively. The results indicate that two sites of Sr^{2+} are substituted by Eu^{2+} in $Sr_3Y(PO_4)_3$, namely, there are two different luminescent sites of Eu^{2+}[11].

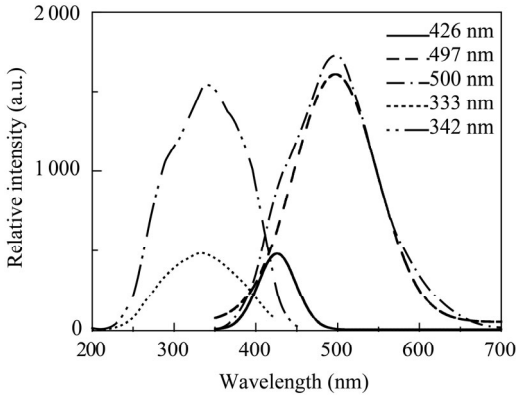

Fig.2 Emission and excitation spectra of $Sr_3Y(PO_4)_3$: $0.01Eu^{2+}$ and decomposed Gaussian profiles

To further validate the different luminescent sites of Eu^{2+}, we investigate the lifetime of Eu^{2+}. As shown in Fig.3, the decay curves of $Sr_3Y(PO_4)_3$:$0.01Eu^{2+}$ excited at 350 nm and monitored at 426 nm and 497 nm are presented, respectively. The decay curves can be well fitted with a second-order exponential decay mode as[11]

$$I=A_1\exp(-t/\tau_1)+A_2\exp(-t/\tau_2), \quad (1)$$

where I is the luminescence intensity, A_1 and A_2 are constants, t is the time, and τ_1 and τ_2 are the lifetimes for the rapid and slow decays, respectively. The average lifetime can be calculated as[11]

$$\tau^*=(A_1\tau_1^2+A_2\tau_2^2)/(A_1\tau_1+A_2\tau_2). \quad (2)$$

For $Sr_3Y(PO_4)_3$:$0.01Eu^{2+}$, the lifetime values are determined to be 0.362 μs and 0.469 μs, which correspond to the emissions at 426 nm and 497 nm, respectively. Two types of Eu^{2+} luminescent centers in $Sr_3Y(PO_4)_3$ should be related to the crystallographic sites and the crystal structure. Furthermore, according to the report of Van Uitert[13], the emission position of Eu^{2+} is strongly dependent on its local environment, which is suggested to obey the experimental equation as

$$E=Q[1-(V/4)^{1/V}\times 10^{-(n\times Ea\times r)/80}], \quad (3)$$

where E is the position of the d-band edge in energy for the rare-earth ion, Q represents the position of the lower d-band edge in energy for the free ion, V is the valence of the active cation, n is the number of anions in the immediate shell around the active cation, E_a is the electron affinity of the atoms from anions, which is different when Eu^{2+} is introduced into different anion complexes with various CNs, and r is the radius of the host cation (Sr^{2+}) replaced by the active cation (Eu^{2+}). Here, E_a with unit of eV is constant for the same host, Q=34 000 cm^{-1} for Eu^{2+}, V=2 for Eu^{2+}, and E with unit of cm^{-1} is proportional to the product of n and r. On the basis of this, which kind of crystallographic site is substituted by Eu^{2+} in $Sr_3Y(PO_4)_3$ can be investigated theoretically in this paper. According to Ref.[11], the effective ionic radii of two Sr^{2+} ions are r=0.131 nm for CN=9 and r=0.116 nm for CN=6. Therefore, we can conclude that the emission peak centered at 426 nm is attributed to Eu^{2+} occupying the nine-coordination Sr^{2+} site, and the other peak centered at 497 nm is attributed to Eu^{2+} ion occupying the six-coordination Sr^{2+} site.

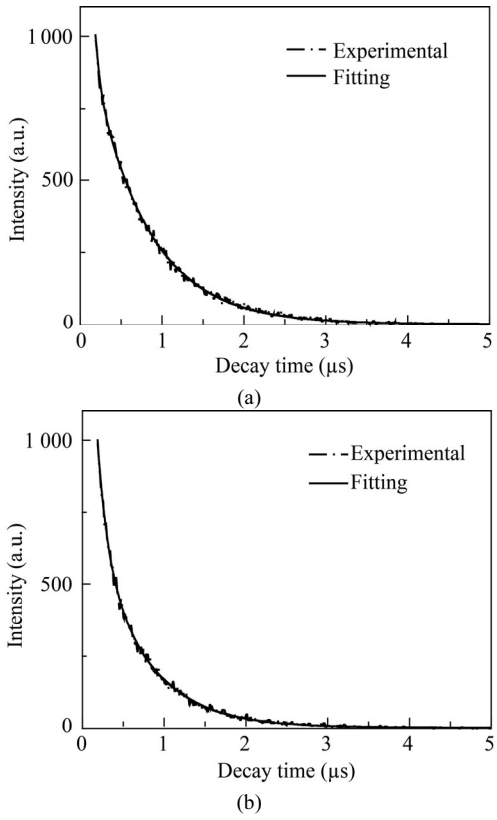

Fig.3 PL decay curves of Eu^{2+} in $Sr_3Y(PO_4)_3$:0.01Eu^{2+} excited at 350 nm monitored at (a) 426 nm and (b) 497 nm

Fig.4 presents the emission spectra of $Sr_{3-x}Y(PO_4)_3$:xEu^{2+} (x=0.005, 0.01, 0.02, 0.03 and 0.05). It can be obviously observed that the emission at 426 nm gradually weakens till disappears with the increase of Eu^{2+} doping content, while the emission at 497 nm always exists. The inset of Fig.4 shows the Eu^{2+} content depends on the emission intensity corresponding to the two peaks at 426 nm and 497 nm, respectively. It can be easily seen that the emission intensities at 426 nm and 497 nm both increase and reach the maximum at x=0.01, and then the emission intensities decrease. This means that the part of energy for Eu^{2+} with CN=9 may transfer to Eu^{2+} with CN=6. Moreover, the variations of the two emission centers are both caused by the internal concentration quenching effect, so the interaction type between sensitizers or between sensitizer and activator can be expressed as[14]

$$I/x=k[1+\beta(x)^{\theta/3}]^{-1}, \quad (4)$$

where k and β are constants for each type of interaction for a given host lattice, x is the activator content which is larger than the critical concentration, I/x is the emission intensity per activator content for a given host crystal, and θ is an indication of electric multipolar characteristic. Here, θ=6, 8 and 10 correspond to dipole-dipole (d-d), dipole-quadrupole (d-q) and quadrupole-quadrupole (q-q) interactions, respectively. Fig.5 depicts the fitting lines of $\log(I/x)$ versus $\log(x)$ in $Sr_{3-x}Y(PO_4)_3$:xEu^{2+} for the different emission peaks of 426 nm and 497 nm. $\log(I/x)$ shows a relatively linear dependence on $\log(x)$, and the slopes are determined to be –1.924 04 and –3.294 68 for 426 nm and 497 nm, respectively. θ can be calculated as 5.77 and 9.88, respectively. Based on a minor approximation, 5.77 is close to 6, which means that the quenching is d-d interaction for Eu^{2+} center with CN=9. As a comparison, the calculated θ of 9.88 is close to 10, which means that the quenching is q-q interaction for Eu^{2+} center with CN=6.

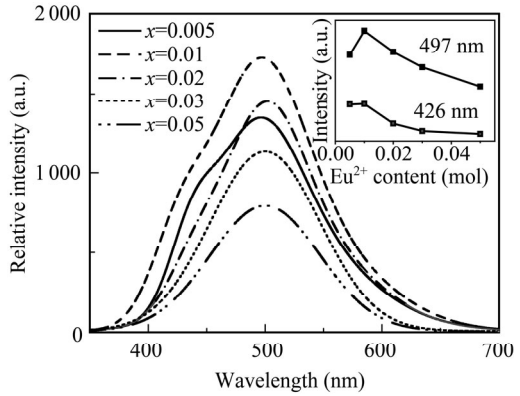

Fig.4 Emission spectra of $Sr_{3-x}Y(PO_4)_3$:xEu^{2+} (The inset is the emission intensity of $Sr_{3-x}Y(PO_4)_3$:xEu^{2+} as a function of Eu^{2+} doping content.)

To investigate the concentration quenching phenomena of the phosphor, the crystal distance R_c between Eu^{2+} ions can be estimated by[15]

$$R_c\approx 2[3V/(4\pi x_c N)]^{1/3}, \quad (5)$$

where x is the concentration of Eu^{2+}, N is the number of Z ions in the unit cell (N=4 for $Sr_3Y(PO_4)_3$), and V is the

volume of the unit cell (V≈1.033 1 nm^3). In this case, the critical doping content of Eu^{2+} in $Sr_3Y(PO_4)_3$ is 0.01. As a result, R_c of Eu^{2+} in $Sr_3Y(PO_4)_3$ is approximately 3.67 nm.

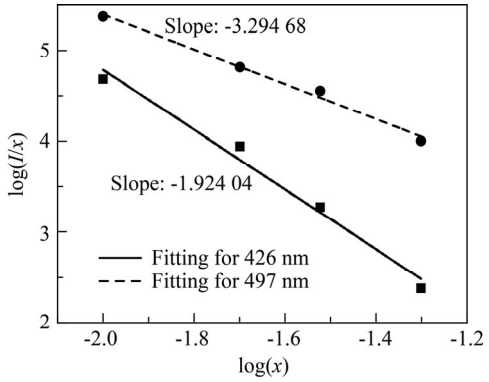

Fig.5 The fitting lines of log(*I*/*x*) versus log(*x*) in $Sr_3Y(PO_4)_3:Eu^{2+}$ with emission peaks of 426 nm and 497 nm

Under the UV light at 365 nm, the CIE chromaticity of $Sr_{3-x}Y(PO_4)_3:xEu^{2+}$ (x=0.005, 0.01, 0.02, and 0.03) is measured and shown in Fig.6. For $Sr_{3-x}Y(PO_4)_3:xEu^{2+}$, CIE($x$, y) coordinates systematically shift from cyan to green region with the increase of Eu^{2+} doping content. The results also prove that the two different Eu^{2+} luminescence centers can be adjusted by Eu^{2+} doping content.

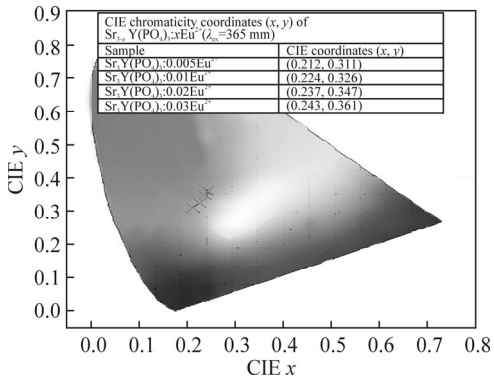

Fig.6 CIE chromaticity coordinates (*x*, *y*) of $Sr_{3-x}Y(PO_4)_3:xEu^{2+}$ with λ_{ex}=365 nm

In summary, a series of $Sr_3Y(PO_4)_3:Eu^{2+}$ samples are synthesized by the conventional solid-state method. Under the radiation excitation at 350 nm, $Sr_3Y(PO_4)_3:Eu^{2+}$ shows an asymmetrical emission band, which indicates that two sites of Sr^{2+} are substituted by Eu^{2+} in host. The emissions at 426 nm and 497 nm are attributed to Eu^{2+} ion occupying the nine-coordination Sr^{2+} and the six-coordination Sr^{2+}, respectively. The emission color of $Sr_3Y(PO_4)_3:Eu^{2+}$ can be adjusted from cyan to green with the increase of Eu^{2+} doping content, its emission intensity can be also tuned, and the concentration quenching effect is observed. For two Eu^{2+} ions with CN=9 and 6, the quenching mechanisms are d-d and q-q interactions, respectively, and the critical distance of energy transfer is calculated by concentration quenching and turns out to be about 3.67 nm. All the results above show that the wavelength peaks at 426 nm and 497 nm in $Sr_3Y(PO_4)_3:Eu^{2+}$ originate from two different Eu^{2+} luminescence centers in the lattice.

References

[1] Wang T., Zheng P., Liu X., Chen H., Bian L. and Liu Q. L., J. Lumin. **47**, 173 (2014).
[2] Chen W.-T., Sheu H.-S., Liu R.-S. and Attfield J. P., J. Am. Chem. Soc. **134**, 8022 (2012).
[3] Tian Hua, Song Jun, Lu Qi-fei and Wang Da-jian, Optoelectronics Letters **8**, 352 (2012).
[4] Li Jian, Deng Jia-chun, Lu Qi-fei and Wang Da-jian, Optoelectronics Letters **9**, 293 (2013).
[5] Yadav R. S., Shukla V. K., Mishra P., Pandey S. K., Kumar K., Baranwal V., Kumar M. and Pandey A. C., J. Alloys Compd. **547**, 1 (2013).
[6] Pang Li-bin, Gao Shao-jie, Gao Zhan-jun, Li Hong-lian and Wang Zhi-jun, Optoelectronics Letters **9**, 282 (2013).
[7] Kuo T. W. and Chen T. M., J. Electrochem. Soc. **157**, J216 (2010).
[8] Guo N., Lü W., Jia Y., Lv W. and Zhao Q., Physical Chemistry Chemical Physics **14**, 192 (2013).
[9] Jia Y., Lü W., Guo N., Lü W., Zhao Q. and You H., Physical Chemistry Chemical Physics **15**, 6057 (2013).
[10] Sun J., Sun Y., Zeng J. and Du H., Opt. Mater. **35**, 1276 (2013).
[11] Guo N., Huang Y., Yang M., Song Y., Zheng Y. and You H., Physical Chemistry Chemical Physics **13**, 15077 (2011).
[12] Shannon R. D., Acta Cryst. **A32**, 751 (1976).
[13] Van Uitert L. G., J. Lumin. **29**, 1 (1984).
[14] Van Uitert L. G., J. Electrochem. Soc. **114**, 1048 (1967).
[15] Blasse G., Philips Res. Rep. **24**, 131 (1969).